

---

# THE EMERGENCE OF COMPLEX BEHAVIOR IN LARGE-SCALE ECOLOGICAL ENVIRONMENTS

**Joseph Bejjani\***  
Harvard University

**Chase Van Amburg**  
Harvard University

**Chengrui Wang**  
Fudan University

**Chloe Huangyuan Su**  
Harvard University

**Sarah M. Pratt**  
University of Washington

**Yasin Mazloumi**  
Harvard University

**Naeem Khoshnevis**  
Harvard University

**Sham M. Kakade**  
Harvard University

**Kianté Brantley**  
Harvard University

**Aaron Walsman\***  
Harvard University

## ABSTRACT

We explore how physical scale and population size shape the emergence of complex behaviors in open-ended ecological environments. In our setting, agents are unsupervised and have no explicit rewards or learning objectives but instead evolve over time according to reproduction, mutation, and natural selection. As they act, agents also shape their environment and the population around them in an ongoing dynamic ecology. Our goal is not to optimize a single high-performance policy, but instead to examine how behaviors emerge and evolve across large populations due to natural competition and environmental pressures. In an effort to discover how complex behaviors naturally emerge, we conduct experiments in large-scale worlds that reach populations of more than 60,000 individual agents, each with their own evolved neural network policy. We identify various emergent behaviors such as long-range resource extraction, vision-based foraging, and predation that arise under competitive and survival pressures. We examine how sensing modalities and environmental scale affect the emergence of these behaviors, finding that some appear only in sufficiently large environments and populations, with larger scales increasing behavioral stability and consistency. While there is a rich history of research in evolutionary settings, our scaling results provide promising new directions to explore ecology as an instrument of machine learning in an era of abundant computational resources. Experimental code is available at <https://github.com/jbejjani2022/ecological-emergent-behavior>.

## 1 INTRODUCTION

Since Darwin, the evolutionary emergence of biodiversity and complex behavior has been studied across a wide variety of biological disciplines, including evolutionary theory (Darwin, 1859; Simpson, 1944), ecology (MacArthur & Wilson, 2001), and genetics (Dobzhansky, 1937). Models of these emergent dynamics range from theories of speciation and adaptive radiation (Coyne & Orr, 2004; Schlüter, 2000) to the mathematical analyses of population genetics (Fisher, 1930; Wright, 1931).

In these fields, decades of mathematical modeling, laboratory experiments, and field work have tremendously improved our understanding of the mechanisms of evolution in nature. Unfortunately, there are many obstacles to studying emergent behavior in the natural world. As ecosystems become larger and more complex, they are more difficult to control and measure. Even where possible, running controlled experiments in large-scale natural settings risks damaging or displacing wild populations.

In an effort to better understand the emergence of complex behavior due to competitive and environmental pressures, we study the open-ended evolution of neural network policies in large-scale

---

\*Correspondence to: [jbejjani@college.harvard.edu](mailto:jbejjani@college.harvard.edu) / [aaronwalsman@fas.harvard.edu](mailto:aaronwalsman@fas.harvard.edu)

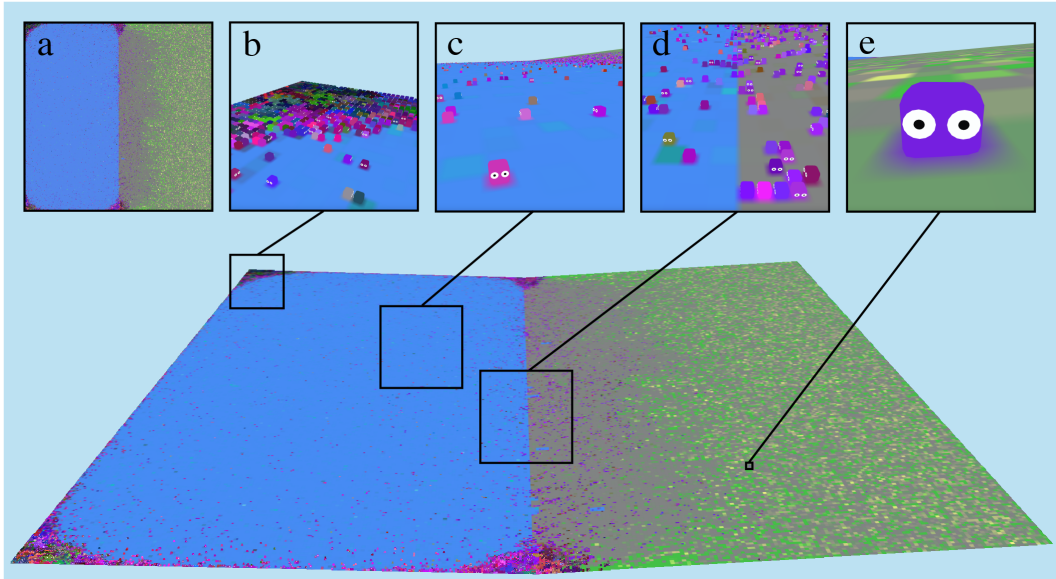


Figure 1: A 3D visualization of a  $512 \times 512$  map in our environment. Insert (a) shows a top down view of the entire map, (b) shows a group of agents clustered in the corner, (c) shows agents in the water, (d) shows agents travelling back and forth from the land and (e) shows a close up of a single agent gathering resources.

ecological simulations. In this setting, agents do not have a specified objective or reward signal but instead collect resources to survive and reproduce according to the dynamics of the environment. Policy changes occur only via mutation as parents pass their policies on to their children. With the rapid growth in computational resources available to researchers, our goal is to study open-ended evolutionary dynamics in populations of these simple digital organisms at scales not previously possible, in the hopes of providing new tools for investigating the effects of environmental scale and population size on behavioral emergence.

To study this, we use a new JAX-based simulation environment (Wang et al., 2025) that allows rapid evaluation of large grid worlds. Our larger experiments can contain over 60,000 individual agents with a physical area of 1,000,000 grid cells. Agents in this environment must navigate to find food and other resources in order to survive. Agents can also reproduce by collecting enough resources to make a mutated copy of themselves. A 3D visualization of this environment can be found in Figure 1.

We identify multiple instances where sensor configurations and large environmental scales strongly impact the resulting behaviors, which can lead to long-term ecological consequences. For example, we show that agents with simple compass sensors can adapt to conduct long-range resource gathering expeditions, but that this behavior emerges less reliably at small scales. We also show that agents with vision sensors will evolve better foraging and attacking behavior than agents without them. Again, these effects are more consistent at large scales.

These investigations aim not only to better understand ecological phenomena through simulation, but also to create a novel environment for studying machine intelligence. Recent years have demonstrated that in AI, scale doesn't merely improve models — it fundamentally transforms their capabilities (Wei et al., 2022a). Yet despite this insight, many attempts at embodied learning have remained confined to simple environments with small populations over short timescales. Our work explores what capabilities emerge when we scale not just a single model but an entire ecosystem. Just as reasoning emerges in individual models only beyond a certain size threshold (Wei et al., 2022b), we ask: what strategies become learnable within populations only when environmental complexity reaches sufficient richness? Through this lens, we present our work not only as a method to learn about ecology, but as an exploration of how ecology itself learns.

---

## 2 RELATED WORK

The emergence of life has inspired computational research since the field’s inception. Conway’s Game of Life (Games, 1970) simulates populations through simple local rules. Early computer programs such as Tierra (Ray, 1992) and Avida (Brown) simulate life as self-replicating programs that evolve through mutations. Like Conway, Reynolds (1987) used local rules of motion to produce emergent flocking and schooling behaviors.

As computers became more powerful, so did the ability to create complex simulations of evolution. Lenia (Chan, 2018; 2020; 2023) generalized the discrete state grid of Conway’s Game of Life into a continuous state space, generating diverse and lifelike organisms. Prior work has evolved agent morphology for locomotion (Sims, 1994a;b; Ha, 2018; Gupta et al., 2021; Auerbach et al., 2014; Auerbach & Bongard, 2012; Jeon et al., 2025; Auerbach & Bongard, 2014; Szerlip & Stanley, 2013), sensing (Pratt et al., 2022; Mugan & MacIver, 2020; Tiwary et al., 2025), and appearance (Mordvintsev et al., 2020), while neuroevolution methods have evolved neural network architectures directly (Stanley & Miikkulainen, 2002; 2004; Stanley et al., 2009).

Evolution has also provided inspiration for the internal dynamics of optimization algorithms. Genetic algorithms (Holland, 1992; Jong, 1975) and evolutionary strategies (Wierstra et al., 2014; Hansen & Ostermeier, 2001; Rechenberg, 1973; Schwefel, 1995; Conti et al., 2018) apply the principles of evolution and natural selection to optimization and have been used to optimize neural networks for tasks like Atari games and Mujoco locomotion tasks (Salimans et al., 2017; Such et al., 2017; Mania et al., 2018). However, these works all use evolution and mutation to optimize agents for a fixed objective and rarely consider populations of agents that directly interact with each other.

There is also a rich history of work more similar to ours, which focuses on observing the evolution of populations within simulated environments not to reach predetermined objectives, but to discover what behaviors naturally emerge from different environmental conditions. Early examples include Bedau (1992), Yaeger et al. (1994), Channon & Damper (1998), and Tisue et al. (2004). More recently, Yamada et al. (2020) study predator-prey dynamics in multi-agent populations using reinforcement learning. Eco (Hamon et al., 2023) and JaxLife (Lu et al., 2024) are recent examples with resources and reproducing agents much like our setting, though at a considerably smaller scale. The Bibites (Caussan, 2025) is an online game and artificial life environment featuring open-ended evolution of agents with simple neural networks. Mordatch & Abbeel (2018) and Park et al. (2023) use simulated environments to investigate the emergence of language and communication between agents. The emergence of behavior due to autocurricula (Leibo et al., 2019), the idea that populations of agents provide an increasingly challenging learning landscape for each other, has also been explored in environments with smaller populations (Leibo et al., 2018; Baker et al., 2019; Team et al., 2021).

Our work also takes inspiration from the many large-scale, high-quality simulators and games that have been developed for single-agent and multi-agent reinforcement learning in recent years (Petrovenco et al., 2021; Jaderberg et al., 2019; Suarez et al., 2019; Zheng et al., 2017; Lechner et al., 2023; Koyamada et al., 2023; Matthews et al., 2024). Other recent large-scale simulators use cellular automata to grow organisms rather than directly evolving agent behavior (Mordvintsev et al., 2020; Robinson, 2021; Heinemann, 2021; Randazzo & Mordvintsev, 2023).

Our goal in this work is to explore open-ended evolution of behavior in an ecological setting at a level of scale and complexity comparable to that of these recent large-scale reinforcement learning environments, while studying the ways that this new scale impacts the resulting emergent behavior.

## 3 METHOD

### 3.1 ECOLOGICAL GAMES

We model the interactions between populations of agents and their environment as a type of multiplayer game we refer to as an **Ecological Game (EG)**. Similar to mathematical models such as Markov decision processes (MDPs) in reinforcement learning and stochastic games (SGs) in multi-agent reinforcement learning (see Sutton et al. (1998) and Albrecht et al. (2024) for reference), an

---

EG contains underlying Markovian transition dynamics but is designed to express changing populations of agents in an objective-free setting. Like an SG, an EG contains a set of players  $\mathcal{G}_t$  at each time point, a state space  $S$ , an initial state distribution  $\rho_0$ , an action space  $A$ , and a transition function  $\mathcal{T}$  mapping states  $s_t$  and a set of actions for each player  $a_{t,i}$  to a distribution over subsequent states  $s_{t+1}$ . Unlike an SG, it adds a population function  $\Gamma(s_t)$  that provides information about which agents are currently alive and the identity of their parents so that birth and death events can be inferred. Just as MDPs and SGs have partially observable counterparts, POMDPs and POSGs, an EG can also be partially observable, in which case we refer to it as a POEG.

### 3.2 ENVIRONMENT

The particular POEG used in our experiments is a large grid world containing various resources that agents must collect in order to reproduce and survive. The environment maintains a factored state space  $s_t = \{s_t^m, s_t^a\}$  where  $s_t^m$  is 2D data associated with the map, such as the terrain and distribution of resources, and  $s_t^a$  is data associated with the agent, such as its position, health, and internal resources.

**Terrain:** Each map has a rock layer defining the height of each grid cell. Maps also include water, which is initially added to grid cells with a rock value below a preset sea-level. Throughout an episode, water flows downhill using a discrete flow simulation. In the experiments below, we use six global terrain configurations shown in Figure 2: **Ocean**, **Beach**, **Island**, **Lake**, **Isthmus**, and **Channel**. We conduct experiments at  $64 \times 64$ ,  $256 \times 256$ ,  $512 \times 512$ , and  $1024 \times 1024$  grid sizes. When growing or shrinking the grid size, we also scale the initial population size proportional to the area change of the overall grid. Once the simulation begins running, the population then fluctuates according to the dynamics of the environment.

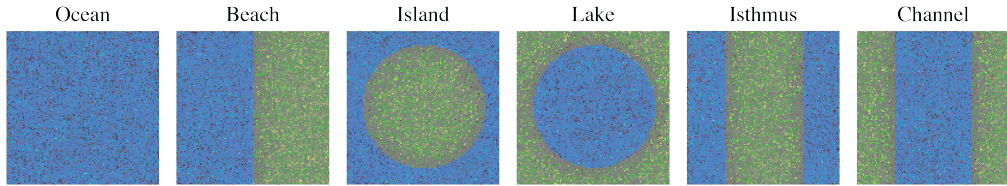


Figure 2: Overhead images of the terrains used in our experiments at  $256 \times 256$  grid size. Small dark spots represent individual agents, while green and yellow represent concentrations of energy and biomass. These images were each captured 5000 steps into an episode after most biomass in the water has been eaten, but before the agents have evolved to survive on land for longer periods.

**Resources and Agent Health:** Agents must collect **water**, **energy**, and **biomass** to survive and reproduce in these environments. Initially, biomass and energy are distributed randomly throughout the environment but can be consumed and redistributed by individual agents.

Each action an agent takes expends a small amount of energy and water. The spent water returns to the landscape, where it flows downhill to the nearest body of water, while the energy is used up and destroyed. Biomass is used for reproduction; all agents require a fixed amount of biomass to exist and therefore cannot reproduce until they have collected enough excess biomass to donate to their offspring. Like water, the total biomass remains constant in the environment throughout the simulation, but unlike water, the biomass does not flow downhill or move on its own. Energy is not held constant but slowly grows on free-standing biomass. We designed these resource dynamics to provide agents with a slightly more challenging problem than collecting a single food source.

Agents also have health points (HP) that they must maintain in order to avoid death. If an agent overspends a critical resource, their health will rapidly deteriorate, but they may use energy and water to slowly recover HP over time. Agents may also attack other agents, reducing the targets' HP. They also take a small but increasing amount of damage based on their age, meaning that agents eventually die of old age if not by other causes. When an agent's HP goes to zero and they die, whatever resources they were carrying are returned to the environment in the grid cell they were standing on. In this way, if an agent attacks and kills another agent, it may then consume their resources as a basic form of predation.

---

**Sensors:** Agents sense the environment using four sensors. The **internal** sensor tells the agent about its age, health, and the resources it is carrying; the **external** sensor detects external resources in the same grid cell as the agent; a **compass**, inspired by the magnetoreceptors found in birds and other animals, detects the agent’s global direction as a 4-way one-hot vector; and **vision** provides a  $7 \times 7$  top-down rendered patch around the agent, containing three color channels as well as a fourth channel showing the local difference in elevation.

**Actions:** Agents have a finite set of discrete actions grouped into five categories. The first is **Rest**, which does nothing but costs the least energy. There are three **Move** actions: rotate clockwise, rotate counterclockwise, and move forward one grid cell. Multiple agents cannot occupy the same cell; if an agent tries to move into the same cell as another agent, or if two agents try to move to the same cell, their move action is canceled. The agents also have a single **Attack** action which kills all agents in the  $3 \times 3$  square directly in front of them. There are three separate **Eat** actions, one for each of the resource types. If an agent is in the same cell as a particular resource, taking the corresponding eat action will transfer a fixed amount of that resource from the environment to the agent’s stomach, which has a fixed maximum capacity.

Finally, agents have a single **Reproduce** action that creates a new offspring via single-parent reproduction. This action is only successful if the agent has accumulated enough resources to donate to its new child. The newly created agent is created directly behind its parent. The child’s policy contains a mutated copy of its parent’s weights. The child also immediately inherits a fixed amount of its parent’s resources.

In the experiments below, we often disable certain sensors or the attack action in order to test the ecological effects of agents with different abilities. We use three agent sensing combinations: internal+external resources only (**R**), internal+external+compass (**RC**), and internal+external+compass+vision (**RCV**). We use **+A** to note when attacking is allowed; for example (**RC+A**) indicates the agent has resource sensors, a compass, and can attack.

### 3.3 POLICIES AND TRAITS

Our agent policies are implemented as small, memoryless MLPs. The raw values for each sensor are flattened, normalized to the range  $[-1, 1]$  and fed through separate linear layers with an output dimension of 64. These values are summed and fed through a 2-layer MLP with hidden dimension 64 and ReLU nonlinearities. The action space is discrete, so the final output is a linear layer with an output dimension equal to the number of possible actions. Actions are sampled from a softmax distribution with a temperature that is allowed to evolve with the network weights. Weights are represented using half-precision bfloat16 values to support larger population sizes and faster run times. Depending on the number of sensors an agent is using, the network size for each agent is between 10k-25k parameters.

In all runs, the weights for the initial population of agents use Kaiming initialization (He et al., 2015); bias vectors are initialized to zero. Policies for agents born in the middle of an episode are created by copying their parent’s weights and applying Gaussian noise with standard deviation  $3 \times 10^{-2}$  to all mutable weight values. This mutation approach is similar to that used in other neuroevolution research (Such et al., 2017). Empirically, we found that a larger mutation rate was necessary due to the use of low-precision floating-point numbers.

Agents also have a 3-channel trait controlling their color when they are rendered onto the map for visual sensing. This color mutates similarly to the network weights.

### 3.4 COMPUTATION AND REPRODUCIBILITY

Our environments and algorithms run on Nvidia H100 and A40 GPUs and are implemented using JAX (Bradbury et al., 2018) to take advantage of parallel computation. Running time depends on configuration parameters, with our largest runs taking several hours to compute 2M steps. For example, a typical run with a grid size of  $512 \times 512$ , a maximum population of 32768, and a 10k parameter model for each agent runs at approximately 190hz on an H100, meaning that a 2M step run for a single seed takes approximately 3 hours.

---

Due to the large and highly randomized nature of these environments, there can be substantial differences in the precise outcomes of each experiment from run to run. As a result, we report the results of four different random seeds for each experiment. Unfortunately, due to nondeterminism in some low-level GPU operations, we find that repeating an experiment with the same random seed does not reliably produce the same results. Despite this, clear high-level patterns emerge when the results of multiple seeds are taken in aggregate. All experiments were run for 2M steps or until extinction unless otherwise noted.

## 4 EXPERIMENTS

In the experiments below, we demonstrate the effects of different sensing modalities, environmental scale, and population size on the emergent behavior of agents.

### 4.1 LONG-DISTANCE RESOURCE GATHERING

In our first experiment, we study the emergent abilities of agents to travel long distances inland in order to find resources. We demonstrate that in environments with clear directional structure, agents with a compass (**RC**) will consistently develop much more effective long-range resource gathering behavior compared to a baseline agent class (**R**) without a compass. We also show that the emergence of this behavior is more consistent and effective at larger environmental scales.

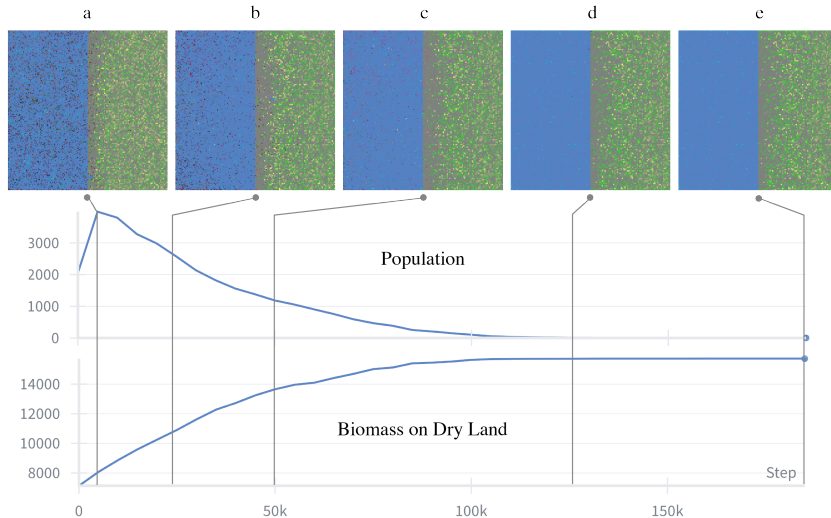


Figure 3: A representative trial with **(R)** agents in a  $256 \times 256$  **Beach** environment. The top chart shows population over time, while the bottom chart shows the free biomass on dry land.

We begin by discussing a visual example of the **(R)** agent class, shown in Figure 3. After 5000 time steps (a), all the initial agents on dry land have died due to lack of water. In the meantime, those in the water have rapidly increased in number due to the rich initial resources. At this early stage, the population does not yet contain sophisticated policies that can efficiently seek out resources. From this early peak in population, agents in the water occasionally stumble onto land (b). When they do, they often cannot find their way back to the ocean and die, depositing their biomass on land. By 50,000 time steps (c), this gradual process has nearly doubled the amount of uneaten biomass on land. This transfer of resources from water to land has caused the population to shrink because there is no longer enough biomass in the water to find in order to reproduce. By 125,000 steps (d), almost all biomass has been transferred to land, and the population is nearly extinct. The final agent dies around 185,000 steps (e).

This example demonstrates the ecological impact of the agents' inability to find their way back to water. Not only do the individuals die, but their deaths alter the distribution of resources in the environment in ways that have important consequences for the entire population. At the same time,

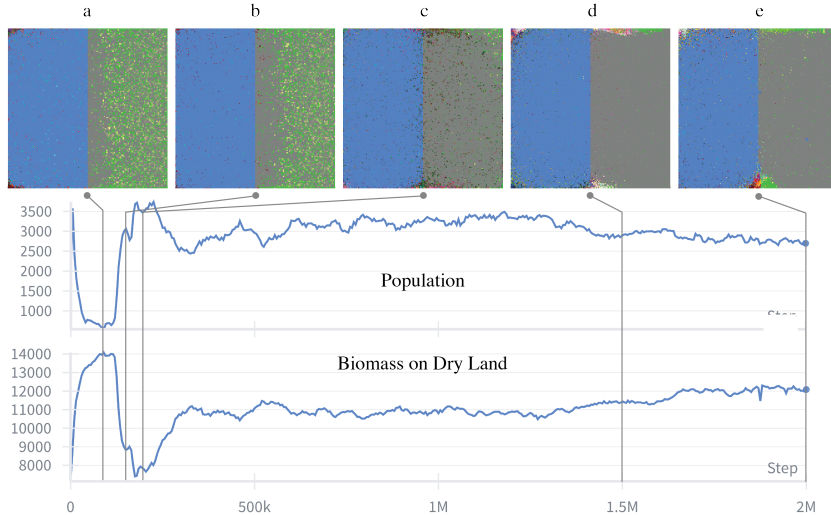


Figure 4: A representative trial with **(RC)** agents in a  $256 \times 256$  **Beach** environment. The top chart shows population over time, while the bottom chart shows the free biomass on dry land.

this ecological catastrophe presents an opportunity for any agent that is able to successfully discover a way to walk onto land, forage in the rich deposits of biomass left by their dead ancestors, and safely return to water.

In the next example, shown in Figure 4, we provide agents with an internal compass **(RC)**. At first, a similar pattern emerges (a) where the population shrinks, and the free biomass on land rapidly increases. However, in this example, some agents are able to use their compass to drift into the relative safety of the corners. At around 150,000 steps (b) some agents start to “mine” the biomass on land, using their compass to navigate back and forth from land to water. By 200,000 steps (c) these miners have cleared the entire beach. The population undergoes minor changes with agents forming clumps around the edges (d) but remains largely stable for the full 2,000,000 time steps (e).

Table 1: Mining and extinction events in the **Beach** terrain among agents with a compass **(RC)** compared to those without a compass **(R)** across five world sizes and initial populations. denotes the number of seeds that featured a mining event. denotes the number of seeds in which the population went extinct before 2M steps. See Table 3 in Appendix A for detailed data from each seed.

|             | 1024 $\times$ 1024<br>32768 | 512 $\times$ 512<br>8192 | 256 $\times$ 256<br>2048 | 128 $\times$ 128<br>512 | 64 $\times$ 64<br>128 |     |
|-------------|-----------------------------|--------------------------|--------------------------|-------------------------|-----------------------|-----|
| <b>(RC)</b> | 4/4                         | 0/4                      | 4/4                      | 0/4                     | 4/4                   | 0/4 |
| <b>(R)</b>  | 1/4                         | 0/4                      | 0/4                      | 4/4                     | 0/4                   | 4/4 |

Our full set of **Beach** experiments uses grid sizes  $1024 \times 1024$ ,  $512 \times 512$ ,  $256 \times 256$ ,  $128 \times 128$ , and  $64 \times 64$ , with initial populations of 32768, 8192, 2048, 512, and 128 agents respectively. We run each experiment with four random seeds and record whether or not mining behavior emerges, which we detect as a drop of at least 10% in the free biomass on dry land. We also record the onset time of the mining event, determined by the local maximum in biomass on land, and the percentage drop in biomass. A summary of mining and extinction events can be found in Table 1 with full details on each seed in Table 3 in Appendix A. Mining behavior consistently emerges in **(RC)** agents compared to **(R)** agents. Mining emerges more consistently in larger environments and occurs in all seeds starting at the  $256 \times 256$  scale. At smaller scales, populations become less stable with a higher likelihood of going extinct earlier on.

---

Table 2: Mining and extinction events in the **Island**, **Lake**, **Isthmus**, and **Channel** terrains among agents with a compass (**RC**) compared to those without a compass (**R**) at the  $512 \times 512$  grid size.  denotes the number of seeds that featured a mining event.  denotes the number of seeds in which the population went extinct before 2M steps. See Table 4 in Appendix A for detailed data from each seed.

|             | Island | Lake | Isthmus | Channel |     |
|-------------|--------|------|---------|---------|-----|
| <b>(RC)</b> | 4/4    | 0/4  | 2/4     | 2/4     | 4/4 |
| <b>(R)</b>  | 3/4    | 1/4  | 2/4     | 4/4     | 1/4 |

We run similar experiments in the **Island**, **Lake**, **Isthmus**, and **Channel** terrains at the  $512 \times 512$  grid size with (**R**) and (**RC**) agents in order to investigate the impact of the terrain configuration on the emergence of mining behavior. Mining and extinction events for these experiments can be found in Table 2, while detailed information about each run can be found in Table 4 in Appendix A. As before, equipping agents with a compass yields earlier and more consistent emergence of mining behavior, as well as more stable populations with lower extinction rates. (**RC**) agents adapt more easily to the island and isthmus environments than to the lake and channel, where they occasionally go extinct. We hypothesize that this is because walking either straight east or west will always take an agent back to water in the island and isthmus, but there is no easy rule like this to follow for the channel and lake. The (**R**) agent cannot reliably adapt to any of these environments, but struggles least on the island. See Figure 10 in Appendix C for a visual of mining in the island terrain.

#### 4.2 VISUAL FORAGING AND PREDATION

We also conduct experiments in the ocean environment to determine whether agents can adapt to use vision sensors to effectively locate free resources or prey on other agents. We compare the performance of (**RCV+A**) agents with resource sensing, a compass, and a  $7 \times 7$  visual sensor against (**RC+A**) agents with only resource and compass sensors.

Figure 5 plots population, biomass utilization, movement actions, and eat actions for agents in  $512 \times 512$  and  $128 \times 128$  grid sizes. Plots for other grid sizes can be found in Figure 7 in Appendix B, and summary statistics of these plots can be found in Table 5 in Appendix A. Biomass utilization is computed as the percentage of the total biomass in the environment that is currently inside the agents. We find that in episodes where agents have vision sensors (red lines), they spend less time moving and more time eating. Additionally, these runs support larger populations and have greater biomass utilization. These dynamics indicate that the agents have adapted to use their visual sensing abilities to forage for food more efficiently. When comparing across environmental scales, we find that the variance between runs decreases substantially in larger environments. Unexpectedly, runs that include vision sensors have much more stable dynamics, with less variation in these metrics over time.

Figure 6 shows the averaged attacks per agent and homicides per attack for these runs. These statistics show that agents with vision attack relatively infrequently, but maintain a successful kill rate of approximately 75%. In large grids, agents without vision sometimes also have high kill rates, though with much more unstable dynamics. Unfortunately, there are confounding factors that make it difficult to determine the underlying causes of this observation. Through visual inspection (see Figure 11 in Appendix C), we have found that sometimes these high kill rates occur when clusters of agents build up in one location, and that these clusters almost never form in runs with visual agents. This may also indicate that agents with vision can adapt to avoid each other. In smaller environments, the difference between visual agents and blind agents is less pronounced, but populations of visual agents remain far more stable.

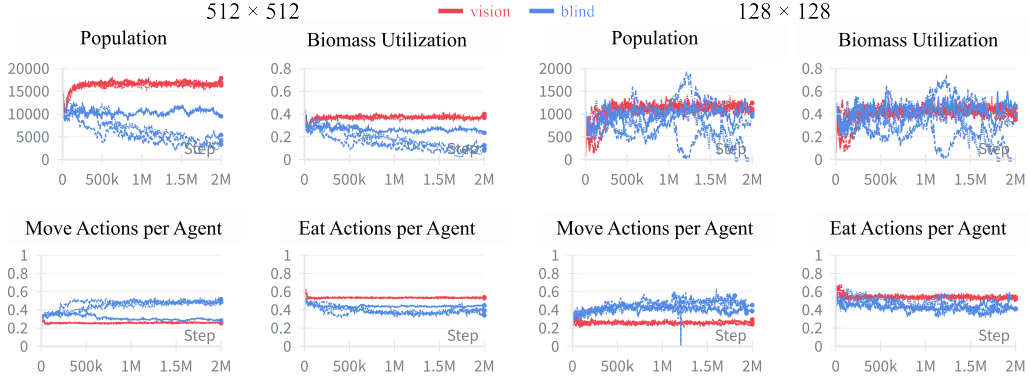


Figure 5: Population, biomass utilization, move actions per agent, and eat actions per agent in a  $512 \times 512$  (left) and  $128 \times 128$  (right) ocean world. Biomass utilization, move actions per agent, and eat actions per agent are averaged across all agents at the time step. Each plot shows four seeds where agents have vision (**RCV + A**) (red) and four seeds where agents are blind (**RC + A**) (blue). With vision, agent populations are larger and more stable, with greater biomass utilization as a result of less moving and more frequent and effective eating. At larger scales, these dynamics are more stable with less variance across runs, suggesting that in larger environments, the vision sensor offers an increasing advantage over not having one for adapting foraging behavior. See Figure 7 in Appendix B for a comparison of grid sizes  $1024 \times 1024$  and  $256 \times 256$ .

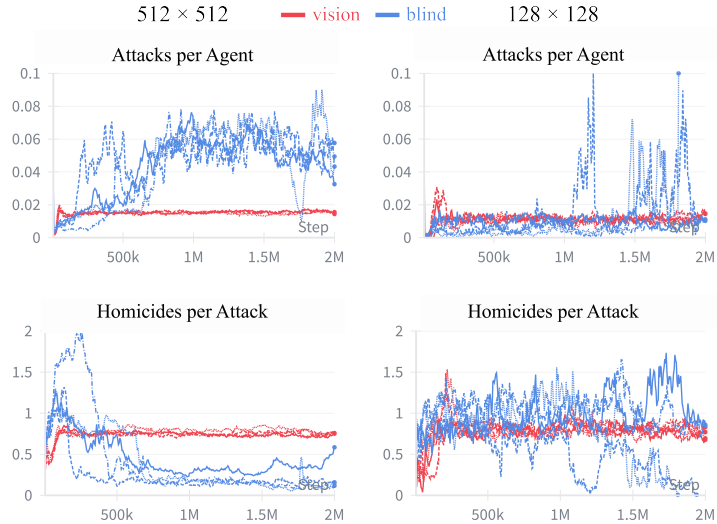


Figure 6: Attacks per agent and homicides per attack, averaged across agents, in a  $512 \times 512$  and  $128 \times 128$  ocean world. Each plot shows four seeds where agents have vision (**RCV + A**) (red) and four seeds where agents are blind (**RC + A**) (blue). With vision, agents attack less frequently but with much higher precision, suggesting the emergence of specialized predation behaviors besides the foraging capabilities demonstrated in Figure 5. Once again, this dynamic is more pronounced at larger scales, with more variance in the behaviors of blind agents at smaller world sizes. See Figure 8 in Appendix B for a comparison of grid sizes  $1024 \times 1024$  and  $256 \times 256$ .

## 5 CONCLUSION

Our study highlights the promise of open-ended evolutionary settings as a powerful paradigm for investigating the emergence of intelligence. Unlike task-driven reinforcement learning, these environments allow agents to evolve behaviors shaped by survival and reproduction in dynamic ecological contexts. Through experiments in grid worlds of varying scale and complexity, we find that

---

both environmental size and sensory richness greatly contribute to the development of sophisticated sensing and decision-making policies. Taken together, these results suggest that ecological and evolutionary pressures, when coupled with rich environments, may provide a natural pathway for the development of increasingly intelligent agents.

## REFERENCES

Stefano V. Albrecht, Filippos Christianos, and Lukas Schäfer. *Multi-Agent Reinforcement Learning: Foundations and Modern Approaches*. MIT Press, 2024. URL <https://www.marl-book.com>.

Joshua Auerbach, Deniz Aydin, Andrea Maesani, Przemyslaw Kornatowski, Titus Cieslewski, Grégoire Heitz, Pradeep Fernando, Ilya Loshchilov, Ludovic Daler, and Dario Floreano. Robogen: Robot generation through artificial evolution. In *Artificial Life Conference Proceedings*, pp. 136–137. MIT Press One Rogers Street, Cambridge, MA 02142-1209, USA journals-info ..., 2014.

Joshua E Auerbach and Josh C Bongard. Environmental influence on the evolution of morphological complexity in machines. *PLoS computational biology*, 10(1):e1003399, 2014.

Joshua E Auerbach and Joshua C Bongard. On the relationship between environmental and morphological complexity in evolved robots. In *Proceedings of the 14th annual conference on Genetic and evolutionary computation*, pp. 521–528, 2012.

Bowen Baker, Ingmar Kanitscheider, Todor Markov, Yi Wu, Glenn Powell, Bob McGrew, and Igor Mordatch. Emergent tool use from multi-agent autocurricula. In *International conference on learning representations*, 2019.

Mark Bedau. Measurement of evolutionary activity, teleology, and life. 1992.

James Bradbury, Roy Frostig, Peter Hawkins, Matthew James Johnson, Chris Leary, Dougal Maclaurin, George Necula, Adam Paszke, Jake VanderPlas, Skye Wanderman-Milne, and Qiao Zhang. JAX: composable transformations of Python+NumPy programs, 2018. URL <http://github.com/jax-ml/jax>.

Chris Adami and C Titus Brown. Evolutionary learning in the 2d artificial life system avida.

Léo Caussan. The bibites: Digital life, 2025. URL <https://www.thebibites.com/>. Artificial life simulation software / game.

Bert Wang-Chak Chan. Lenia-biology of artificial life. *arXiv preprint arXiv:1812.05433*, 2018.

Bert Wang-Chak Chan. Lenia and expanded universe. In *Artificial Life Conference Proceedings 32*, pp. 221–229. MIT Press One Rogers Street, Cambridge, MA 02142-1209, USA journals-info ..., 2020.

Bert Wang-Chak Chan. Towards large-scale simulations of open-ended evolution in continuous cellular automata. In *Proceedings of the companion conference on genetic and evolutionary computation*, pp. 127–130, 2023.

AD Channon and RI Damper. Perpetuating evolutionary emergence. 1998.

Edoardo Conti, Vashisht Madhavan, Felipe Petroski Such, Joel Lehman, Kenneth Stanley, and Jeff Clune. Improving exploration in evolution strategies for deep reinforcement learning via a population of novelty-seeking agents. *Advances in neural information processing systems*, 31, 2018.

Jerry A. Coyne and H. Allen Orr. *Speciation*. Sinauer Associates, Sunderland, MA, 2004.

Charles Darwin. *On the Origin of Species*. John Murray, London, 1859.

Theodosius Dobzhansky. *Genetics and the Origin of Species*. Columbia University Press, New York, 1937.

---

Ronald Aylmer Fisher. *The Genetical Theory of Natural Selection*. Clarendon Press, Oxford, 1930.

Mathematical Games. The fantastic combinations of john conway’s new solitaire game “life” by martin gardner. *Scientific American*, 223:120–123, 1970.

Agrim Gupta, Silvio Savarese, Surya Ganguli, and Li Fei-Fei. Embodied intelligence via learning and evolution. *Nature communications*, 12(1):5721, 2021.

David R Ha. Reinforcement learning for improving agent design. *Artificial Life*, 25:352–365, 2018. URL <https://api.semanticscholar.org/CorpusID:52945447>.

Gautier Hamon, Eleni Nisioti, and Clément Moulin-Frier. Eco-evolutionary dynamics of non-episodic neuroevolution in large multi-agent environments. In *Proceedings of the Companion Conference on Genetic and Evolutionary Computation*, pp. 143–146, 2023.

Nikolaus Hansen and Andreas Ostermeier. Completely derandomized self-adaptation in evolution strategies. *Evolutionary computation*, 9(2):159–195, 2001.

Kaiming He, Xiangyu Zhang, Shaoqing Ren, and Jian Sun. Delving deep into rectifiers: Surpassing human-level performance on imagenet classification. In *Proceedings of the IEEE International Conference on Computer Vision (ICCV)*, pp. 1026–1034, 2015.

Christian Heinemann. Alien. <https://github.com/chrhxh/alien>, 2021.

John H. Holland. Adaptation in natural and artificial systems: An introductory analysis with applications to biology, control, and artificial intelligence. 1992. URL <https://api.semanticscholar.org/CorpusID:58781161>.

Max Jaderberg, Wojciech M Czarnecki, Iain Dunning, Luke Marris, Guy Lever, Antonio Garcia Castaneda, Charles Beattie, Neil C Rabinowitz, Ari S Morcos, Avraham Ruderman, et al. Human-level performance in 3d multiplayer games with population-based reinforcement learning. *Science*, 364(6443):859–865, 2019.

Hyeonseong Jeon, Ainaz Eftekhar, Aaron Walsman, Kuo-Hao Zeng, Ali Farhadi, and Ranjay Krishna. Convergent functions, divergent forms. *arXiv preprint arXiv:2505.21665*, 2025.

Kenneth A. De Jong. An analysis of the behavior of a class of genetic adaptive systems. 1975. URL <https://api.semanticscholar.org/CorpusID:57626488>.

Sotetsu Koyamada, Shinri Okano, Soichiro Nishimori, Yu Murata, Keigo Habara, Haruka Kita, and Shin Ishii. Pgx: Hardware-accelerated parallel game simulators for reinforcement learning. In *Advances in Neural Information Processing Systems*, volume 36, pp. 45716–45743, 2023.

Mathias Lechner, Tim Seyde, Tsun-Hsuan Johnson Wang, Wei Xiao, Ramin Hasani, Joshua Rountree, Daniela Rus, et al. Gigastep-one billion steps per second multi-agent reinforcement learning. *Advances in Neural Information Processing Systems*, 36:155–170, 2023.

Joel Z Leibo, Julien Perolat, Edward Hughes, Steven Wheelwright, Adam H Marblestone, Edgar Duéñez-Guzmán, Peter Sunehag, Iain Dunning, and Thore Graepel. Malthusian reinforcement learning. *arXiv preprint arXiv:1812.07019*, 2018.

Joel Z Leibo, Edward Hughes, Marc Lanctot, and Thore Graepel. Autocurricula and the emergence of innovation from social interaction: A manifesto for multi-agent intelligence research. *arXiv preprint arXiv:1903.00742*, 2019.

Chris Lu, Michael Beukman, Michael Matthews, and Jakob Foerster. Jaxlife: An open-ended agentic simulator. In *Artificial Life Conference Proceedings 36*, volume 2024, pp. 47. MIT Press One Rogers Street, Cambridge, MA 02142-1209, USA journals-info . . . , 2024.

Robert H MacArthur and Edward O Wilson. *The theory of island biogeography*, volume 1. Princeton university press, 2001.

---

Horia Mania, Aurelia Guy, and Benjamin Recht. Simple random search provides a competitive approach to reinforcement learning. *arXiv preprint arXiv:1803.07055*, 2018.

Michael Matthews, Michael Beukman, Benjamin Ellis, Mikayel Samvelyan, Matthew Jackson, Samuel Coward, and Jakob Foerster. Craftax: A lightning-fast benchmark for open-ended reinforcement learning. *arXiv preprint arXiv:2402.16801*, 2024.

Igor Mordatch and Pieter Abbeel. Emergence of grounded compositional language in multi-agent populations. In *Proceedings of the AAAI conference on artificial intelligence*, volume 32, 2018.

Alexander Mordvintsev, Ettore Randazzo, Eyvind Niklasson, and Michael Levin. Growing neural cellular automata. *Distill*, 2020. doi: 10.23915/distill.00023. <https://distill.pub/2020/growing-ca>.

Ugurcan Mugan and Malcolm A MacIver. Spatial planning with long visual range benefits escape from visual predators in complex naturalistic environments. *Nature communications*, 11(1):3057, 2020.

Joon Sung Park, Joseph O'Brien, Carrie Jun Cai, Meredith Ringel Morris, Percy Liang, and Michael S Bernstein. Generative agents: Interactive simulacra of human behavior. In *Proceedings of the 36th annual acm symposium on user interface software and technology*, pp. 1–22, 2023.

Aleksei Petrenko, Erik Wijmans, Brennan Shacklett, and Vladlen Koltun. Megaverse: Simulating embodied agents at one million experiences per second. In *International Conference on Machine Learning*, pp. 8556–8566. PMLR, 2021.

Sarah Pratt, Luca Weihs, and Ali Farhadi. The introspective agent: Interdependence of strategy, physiology, and sensing for embodied agents. *arXiv preprint arXiv:2201.00411*, 2022.

Ettore Randazzo and Alexander Mordvintsev. Biomaker ca: a biome maker project using cellular automata. *arXiv preprint arXiv:2307.09320*, 2023.

Thomas S Ray. Evolution, ecology and optimization of digital organisms. *Santa Fe*, 1992.

Ingo Rechenberg. Evolutionsstrategie : Optimierung technischer systeme nach prinzipien der biologischen evolution. 1973. URL <https://api.semanticscholar.org/CorpusID:60975248>.

Craig W Reynolds. Flocks, herds and schools: A distributed behavioral model. In *Proceedings of the 14th annual conference on Computer graphics and interactive techniques*, pp. 25–34, 1987.

Max Robinson. Life engine. <https://github.com/MaxRobinsonTheGreat/LifeEngine>, 2021.

Tim Salimans, Jonathan Ho, Xi Chen, and Ilya Sutskever. Evolution strategies as a scalable alternative to reinforcement learning. *ArXiv*, abs/1703.03864, 2017. URL <https://api.semanticscholar.org/CorpusID:11410889>.

Dolph Schluter. *The Ecology of Adaptive Radiation*. Oxford University Press, Oxford, 2000.

Hans-Paul Schwefel. Evolution and optimum seeking. In *Sixth-generation computer technology series*, 1995. URL <https://api.semanticscholar.org/CorpusID:43418053>.

George Gaylord Simpson. *Tempo and Mode in Evolution*. Columbia University Press, New York, 1944.

Karl Sims. Evolving virtual creatures. *Proceedings of the 21st annual conference on Computer graphics and interactive techniques*, 1994a. URL <https://api.semanticscholar.org/CorpusID:28435>.

Karl Sims. Evolving 3d morphology and behavior by competition. *Artificial life*, 1(4):353–372, 1994b.

---

Kenneth O Stanley and Risto Miikkulainen. Evolving neural networks through augmenting topologies. *Evolutionary computation*, 10(2):99–127, 2002.

Kenneth O Stanley and Risto Miikkulainen. Competitive coevolution through evolutionary complexification. *Journal of artificial intelligence research*, 21:63–100, 2004.

Kenneth O Stanley, David B D’Ambrosio, and Jason Gauci. A hypercube-based encoding for evolving large-scale neural networks. *Artificial life*, 15(2):185–212, 2009.

Joseph Suarez, Yilun Du, Phillip Isola, and Igor Mordatch. Neural mmo: A massively multiagent game environment for training and evaluating intelligent agents. *arXiv preprint arXiv:1903.00784*, 2019.

Felipe Petroski Such, Vashisht Madhavan, Edoardo Conti, Joel Lehman, Kenneth O Stanley, and Jeff Clune. Deep neuroevolution: Genetic algorithms are a competitive alternative for training deep neural networks for reinforcement learning. *arXiv preprint arXiv:1712.06567*, 2017.

Richard S Sutton, Andrew G Barto, et al. *Reinforcement learning: An introduction*, volume 1. MIT press Cambridge, 1998.

Paul Szerlip and Kenneth Stanley. Indirectly encoded sodarace for artificial life. In *Artificial Life Conference Proceedings*, pp. 218–225. Citeseer, 2013.

Open Ended Learning Team, Adam Stooke, Anuj Mahajan, Catarina Barros, Charlie Deck, Jakob Bauer, Jakub Sygnowski, Maja Trebacz, Max Jaderberg, Michael Mathieu, et al. Open-ended learning leads to generally capable agents. *arXiv preprint arXiv:2107.12808*, 2021.

Seth Tisue, Uri Wilensky, et al. Netlogo: A simple environment for modeling complexity. In *International conference on complex systems*, volume 21, pp. 16–21. Boston, MA, 2004.

Kushagra Tiwary, Aaron Young, Zaid Tasneem, Tzofi Klinghoffer, Akshat Dave, Tomaso Poggio, Dan-Eric Nilsson, Brian Cheung, and Ramesh Raskar. What if eye...? computationally recreating vision evolution. *arXiv preprint arXiv:2501.15001*, 2025.

Chengrui Wang, Chase Van Amburg, Huangyuan Chloe Su, Joseph Bejjani, Yasin Mazloumi, Naeem Koshnevis, Sham Kakade, Kiante Brantley, and Aaron Walsman. DIRT. <https://github.com/aaronwalsman/dirt>, 2025. GitHub repository.

Jason Wei, Yi Tay, Rishi Bommasani, Colin Raffel, Barret Zoph, Sebastian Borgeaud, Dani Yogatama, Maarten Bosma, Denny Zhou, Donald Metzler, et al. Emergent abilities of large language models. *arXiv preprint arXiv:2206.07682*, 2022a.

Jason Wei, Xuezhi Wang, Dale Schuurmans, Maarten Bosma, Fei Xia, Ed Chi, Quoc V Le, Denny Zhou, et al. Chain-of-thought prompting elicits reasoning in large language models. *Advances in neural information processing systems*, 35:24824–24837, 2022b.

Daan Wierstra, Tom Schaul, Tobias Glasmachers, Yi Sun, Jan Peters, and Jürgen Schmidhuber. Natural evolution strategies. *The Journal of Machine Learning Research*, 15(1):949–980, 2014.

Sewall Wright. Evolution in mendelian populations. *Genetics*, 16(2):97–159, 1931.

Larry Yaeger et al. Computational genetics, physiology, metabolism, neural systems, learning, vision, and behavior or poly world: Life in a new context. In *SANTA FE INSTITUTE STUDIES IN THE SCIENCES OF COMPLEXITY-PROCEEDINGS VOLUME-*, volume 17, pp. 263–263. ADDISON-WESLEY PUBLISHING CO, 1994.

Jun Yamada, John Shawe-Taylor, and Zafeirios Fountas. Evolution of a complex predator-prey ecosystem on large-scale multi-agent deep reinforcement learning. In *2020 International joint conference on neural networks (IJCNN)*, pp. 1–8. IEEE, 2020.

Lianmin Zheng, Jiacheng Yang, Han Cai, Weinan Zhang, Jun Wang, and Yong Yu. Magent: A many-agent reinforcement learning platform for artificial collective intelligence. *arXiv preprint arXiv:1712.00600*, 2017.

---

## A ADDITIONAL DATA

Table 3: Mining events in the beach terrain among agents with a compass (**RC**) compared to without a compass (**R**) across five population and world sizes. denotes whether a run had a mining event. denotes the percent decrease in free biomass on dry land during the mining event, and denotes the approximate timestep at which free dry biomass reached the local maximum indicating the start of the mining event. For runs with multiple mining events, we report the first one. denotes the timestep at which the run went extinct, or n/a if it lasted for 2M steps.

| 1024x1024       |                 |      |      | 512x512 |     |       |       | 256x256 |      |      |      | 128x128 |     |     |      | 64x64 |     |      |      |     |
|-----------------|-----------------|------|------|---------|-----|-------|-------|---------|------|------|------|---------|-----|-----|------|-------|-----|------|------|-----|
| 32768           |                 |      |      | 8192    |     |       |       | 2048    |      |      |      | 512     |     |     |      | 128   |     |      |      |     |
| Seed            | Compass On (RC) |      |      |         |     |       |       |         |      |      |      |         |     |     |      |       |     |      |      |     |
|                 | 0               |      | 35k  | 11.1    | n/a |       | 105k  | 33.     | n/a  |      | 145k | 49.3    | n/a |     | 105k | 72.5  | n/a | x    | 55   |     |
| 1               |                 | 90k  | 16.2 | n/a     |     | 50k   | 17.2  | n/a     |      | 50k  | 46.6 | n/a     | x   |     | 140  |       | 70k | 85.3 | 675  |     |
| 2               |                 | 40k  | 15.  | n/a     |     | 30k   | 14.3  | n/a     |      | 55k  | 34.7 | n/a     |     | 50k | 50.7 | n/a   |     | 10k  | 78.  | n/a |
| 3               |                 | 60k  | 15.  | n/a     |     | 45k   | 15.6  | n/a     |      | 90k  | 47.4 | n/a     |     | 20k | 52.  | n/a   | x   |      | 135  |     |
| Avg             | 4/4             | 34k  | 14.3 | 0/4     | 4/4 | 58k   | 20.   | 0/4     | 4/4  | 85k  | 44.5 | 0/4     | 3/4 | 58k | 58.4 | 1/4   | 2/4 | 40k  | 81.7 | 3/4 |
| Compass Off (R) |                 |      |      |         |     |       |       |         |      |      |      |         |     |     |      |       |     |      |      |     |
| Seed            |                 |      |      |         |     |       |       |         |      |      |      |         |     |     |      |       |     |      |      |     |
|                 | 0               | x    |      | n/a     | x   |       | 945k  | x       |      | 185k | x    |         | 65k | x   |      | 45k   |     |      |      |     |
| 1               |                 | 275k | 12.4 | n/a     | x   |       | 1085k | x       |      | 110k | x    |         | 55k | x   |      | 40    |     |      |      |     |
| 2               | x               |      | n/a  | x       |     | 1070k | x     |         | 165k | x    |      | 55k     | x   |     | 25   |       |     |      |      |     |
| 3               | x               |      | n/a  | x       |     | 280k  | x     |         | 125k | x    |      | 90k     | x   |     | 40   |       |     |      |      |     |
| Avg             | 1/4             | 275k | 12.4 | 0/4     | 0/4 |       | n/a   | 0/4     |      | 4/4  | 0/4  |         | 4/4 | 0/4 |      | 4/4   | 0/4 | 4/4  |      |     |

Table 4: Mining events in the island, lake, isthmus, and channel terrains among **(RC)** agents compared to **(R)** agents. Grid size is  $512 \times 512$  with an initial population of 8192.

| Seed | Island          |     |      |     | Lake            |     |      |     | Isthmus         |     |      |     | Channel         |     |      |     |
|------|-----------------|-----|------|-----|-----------------|-----|------|-----|-----------------|-----|------|-----|-----------------|-----|------|-----|
|      | Compass On (RC) |     |      |     | Compass Off (R) |     |      |     | Compass On (RC) |     |      |     | Compass Off (R) |     |      |     |
| 0    | ✓               | 40k | 94.3 | n/a | x               | 45k | ✓    | 45k | 33.             | n/a | ✓    | 50k | 27.4            | n/a |      |     |
| 1    | ✓               | 30k | 94.3 | n/a | ✓               | 30k | 22.5 | n/a | ✓               | 55k | 37.3 | n/a | ✓               | 80k | 30.8 | n/a |
| 2    | ✓               | 30k | 94.8 | n/a | x               | 45k | ✓    | 40k | 28.1            | n/a | ✓    | 50k | 41.             | n/a |      |     |
| 3    | ✓               | 70k | 95.1 | n/a | ✓               | 35k | 25.3 | n/a | ✓               | 30k | 41.5 | n/a | x               |     | 80k  |     |
| Avg  | 4/4             | 43k | 94.6 | 0/4 | 2/4             | 33k | 23.9 | 2/4 | 4/4             | 43k | 35.  | 0/4 | 3/4             | 60k | 33.1 | 1/4 |

| Seed | Island          |      |      |     | Lake            |      |      |       | Isthmus         |     |      |     | Channel         |      |      |  |  |
|------|-----------------|------|------|-----|-----------------|------|------|-------|-----------------|-----|------|-----|-----------------|------|------|--|--|
|      | Compass On (RC) |      |      |     | Compass Off (R) |      |      |       | Compass On (RC) |     |      |     | Compass Off (R) |      |      |  |  |
| 0    | x               | 185k | 185k | x   | x               | 125k | x    | x     | 145k            | x   | x    | x   | x               | 100k |      |  |  |
| 1    | ✓               | 75k  | 30.9 | n/a | x               | 130k | x    | x     | 260k            | x   | x    | x   | x               | 105k |      |  |  |
| 2    | ✓               | 85k  | 47.  | n/a | ✓               | 75k  | 23.4 | 1400k | ✓               | 95k | 18.8 | n/a | x               | x    | 105k |  |  |
| 3    | ✓               | 115k | 39.5 | n/a | ✓               | 70k  | 24.3 | 1250k | x               | x   | 140k | x   | x               | 100k |      |  |  |
| Avg  | 3/4             | 92k  | 39.1 | 1/4 | 2/4             | 73k  | 23.9 | 4/4   | 1/4             | 95k | 18.8 | 3/4 | 0/4             | 0/4  | 4/4  |  |  |

Table 5: denotes population size. denotes biomass utilization, the percentage of total biomass in the system that is currently inside the agents' stomachs. denotes move actions per agent, the fraction of time an agent took a move action, averaged across agents. Similarly, denotes the proportion of agents' actions that were an eat action. Reported values of , , , and are averages of the metric over all steps for the seed.

| Seed | 1024x1024 |      |      |      | 512x512      |      |      |      | 256x256    |      |      |      | 128x128 |      |      |      |
|------|-----------|------|------|------|--------------|------|------|------|------------|------|------|------|---------|------|------|------|
|      | 32768     | 8192 | 2048 | 512  | Vision (RCV) |      |      |      | Blind (RC) |      |      |      |         |      |      |      |
| 0    | 58354     | .396 | .402 | .426 | 16413        | .369 | .257 | .532 | 4195       | .382 | .255 | .536 | 1126    | .426 | .261 | .541 |
| 1    | 65107     | .365 | .257 | .529 | 16200        | .364 | .256 | .533 | 4142       | .377 | .258 | .536 | 1103    | .415 | .262 | .537 |
| 2    | 64735     | .363 | .257 | .530 | 16560        | .372 | .257 | .533 | 4269       | .388 | .260 | .536 | 1041    | .392 | .254 | .542 |
| 3    | 64595     | .362 | .256 | .532 | 16206        | .365 | .255 | .531 | 4249       | .388 | .259 | .533 | 1100    | .414 | .257 | .538 |
| Avg  | 63198     | .371 | .293 | .504 | 16345        | .368 | .256 | .532 | 4213       | .384 | .258 | .535 | 1092    | .412 | .259 | .539 |

| Seed | Island          |      |      |     | Lake            |      |      |       | Isthmus         |     |      |     | Channel         |      |      |  |  |
|------|-----------------|------|------|-----|-----------------|------|------|-------|-----------------|-----|------|-----|-----------------|------|------|--|--|
|      | Compass On (RC) |      |      |     | Compass Off (R) |      |      |       | Compass On (RC) |     |      |     | Compass Off (R) |      |      |  |  |
| 0    | x               | 185k | 185k | x   | x               | 125k | x    | x     | 145k            | x   | x    | x   | x               | 100k |      |  |  |
| 1    | ✓               | 75k  | 30.9 | n/a | x               | 130k | x    | x     | 260k            | x   | x    | x   | x               | 105k |      |  |  |
| 2    | ✓               | 85k  | 47.  | n/a | ✓               | 75k  | 23.4 | 1400k | ✓               | 95k | 18.8 | n/a | x               | x    | 105k |  |  |
| 3    | ✓               | 115k | 39.5 | n/a | ✓               | 70k  | 24.3 | 1250k | x               | x   | 140k | x   | x               | 100k |      |  |  |
| Avg  | 3/4             | 92k  | 39.1 | 1/4 | 2/4             | 73k  | 23.9 | 4/4   | 1/4             | 95k | 18.8 | 3/4 | 0/4             | 0/4  | 4/4  |  |  |

Table 6: denotes attacks per agent, the fraction of time an agent took the attack action, averaged across all agents. The denotes homicides per attack, the number of agents killed per attack action. Reported values of and are averages over all steps for the seed. Note the outlier of 0.562 for of seed 3 in the 128×128 (RC) run. This seed went extinct before 2M steps, resulting in a spike in the attacks per agent metric due to dwindling population size.

|      | 1024x1024    |      | 512x512 |      | 256x256 |       | 128x128    |       |
|------|--------------|------|---------|------|---------|-------|------------|-------|
|      | 32768        | 8192 | 8192    | 2048 | 2048    | 512   | 512        |       |
| Seed | Vision (RCV) |      |         |      |         |       | Blind (RC) |       |
| 0    | .011         | .776 | .015    | .731 | .013    | .784  | .010       | .788  |
| 1    | .016         | .733 | .015    | .741 | .014    | .780  | .011       | .793  |
| 2    | .016         | .707 | .015    | .737 | .014    | .750  | .012       | .771  |
| 3    | .016         | .712 | .015    | .780 | .013    | .759  | .011       | .765  |
| Avg  | .015         | .732 | .015    | .747 | .014    | .758  | .011       | .779  |
|      | Vision (RCV) |      |         |      |         |       | Blind (RC) |       |
| 0    | .070         | .218 | .042    | .437 | .005    | 1.074 | .016       | .558  |
| 1    | .054         | .300 | .044    | .383 | .016    | .871  | .006       | 1.032 |
| 2    | .076         | .236 | .048    | .238 | .031    | .383  | .010       | .979  |
| 3    | .059         | .203 | .044    | .456 | .033    | .446  | .562       | .841  |
| Avg  | .065         | .239 | .045    | .378 | .021    | .693  | .148       | .853  |

## B ADDITIONAL FORAGING AND PREDATION RESULTS

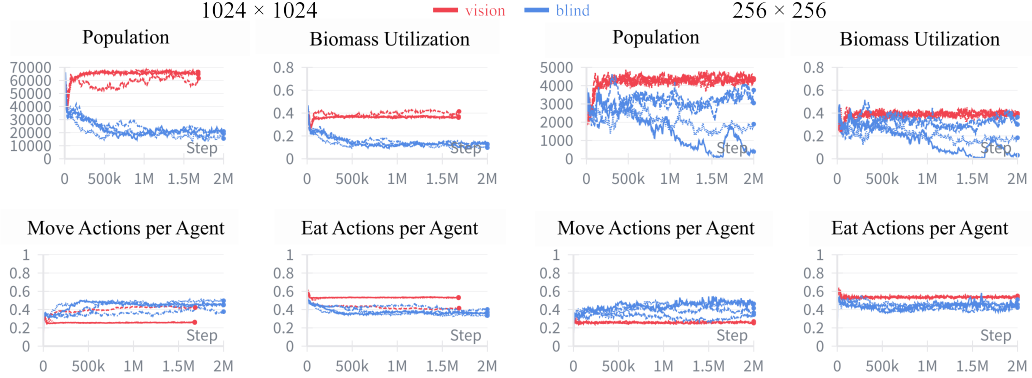


Figure 7: Enabling vision in agents results in more stable populations and greater biomass utilization as a result of more frequent and effective eating and less movement. At larger scales, these dynamics are more stable with less variance across runs. Note that due to limitations on GPU hours, the vision seeds at the  $1024 \times 1024$  scale ran for 1.7M instead of 2M steps.

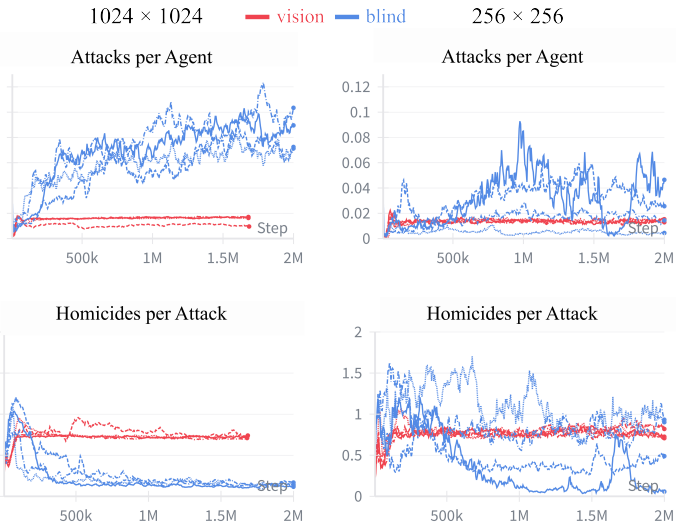


Figure 8: With vision, agents attack less frequently but with much higher precision, suggesting the emergence of specialized predation behaviors in addition to the foraging capabilities demonstrated in Figure 7. Once again, this dynamic is more pronounced at larger scales, with more variance in the behaviors of blind agents in smaller world sizes.

## C ADDITIONAL EXPERIMENTS

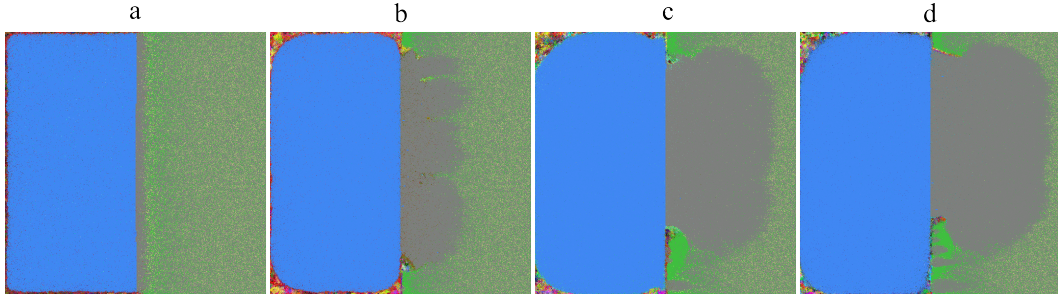


Figure 9: Larger scale environments induce more varied and complex ecologies that give rise to unique visual patterns. In this  $1024 \times 1024$  beach world, **(RC)** agents initially died at the shore (a), transferring biomass to dry land. They then developed mining behavior, clearing biomass from the beach (b). When biomass re-accumulated on the ends of the beach (c), subpopulations of agents re-developed mining behavior, traveling inland on these mini biomass beaches to extract the resources (d).

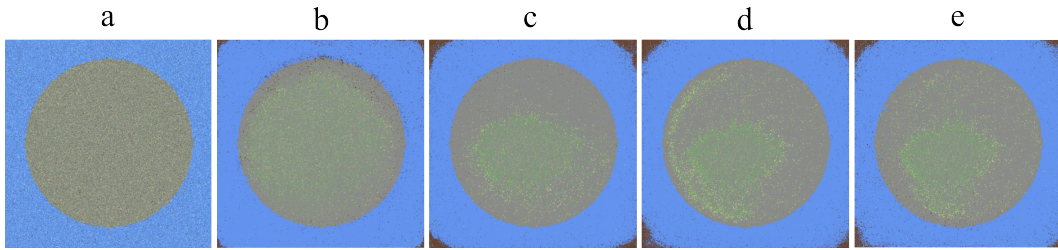


Figure 10: Mining behavior emerges in varied terrains. In this  $512 \times 512$  island world with **(RC)** agents, different regions of the shore are mined throughout the run (b) (c). Biomass is transferred back to parts of the island once mining becomes difficult and agents die before they can return to water (d). Agents adapt to re-mine this wall of accumulated biomass, clearing it from shore (e).

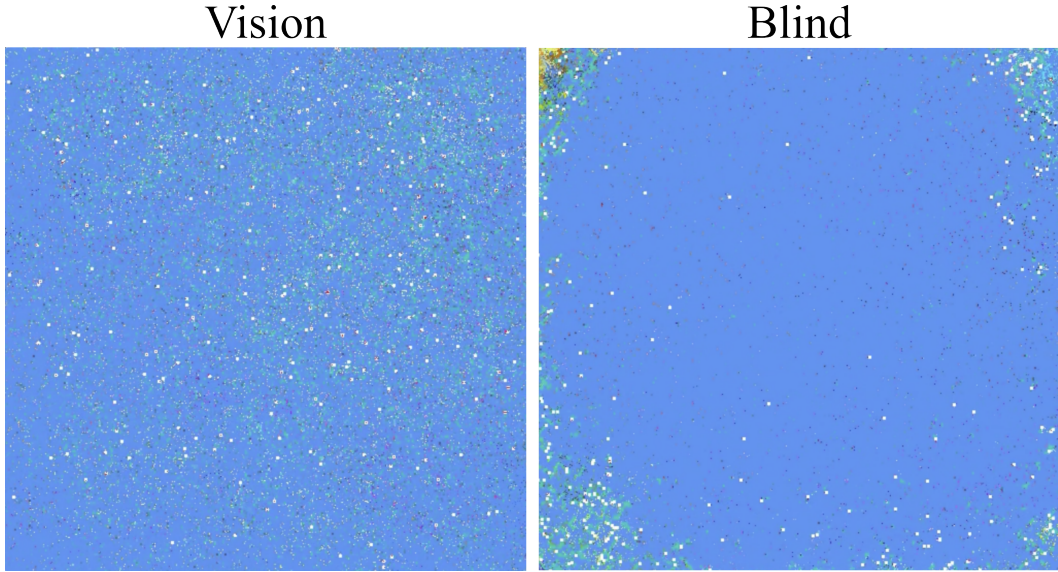


Figure 11: Representative runs in a  $512 \times 512$  ocean terrain where agents have attacking enabled. The white squares in the images indicate an agent is attacking at that location. With vision, agents adapt to locate free resources throughout the ocean world and prey on other agents more effectively (see Figures 5 and 6). Blind agents explore the ocean for resources to a much lesser extent, instead adapting policies for clustering in the corners of the world.